Expanded View Figures

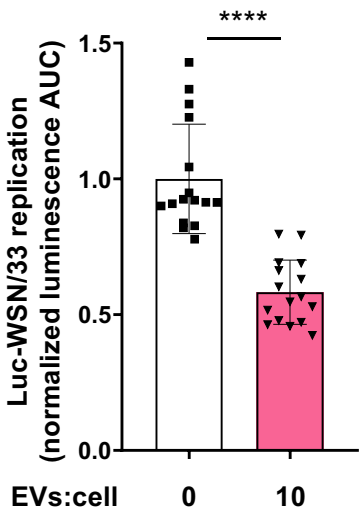

Figure EV1. EVs isolated from immortalized mouse primary peritoneal macrophages inhibit influenza replication.

MDCK-Siat1 cells were co-incubated with Luc-WSN/33 and EVs isolated from immortalized primary mouse peritoneal macrophages. Luc-WSN/33 replication in each condition represented by mean luminescence AUC for individual wells normalized to the mean of the control condition from 4 independent experiments.

Data information: Error bars = SD. Unpaired Student's *t*-test (****P value of < 0.0001).

Source data are available online for this figure.

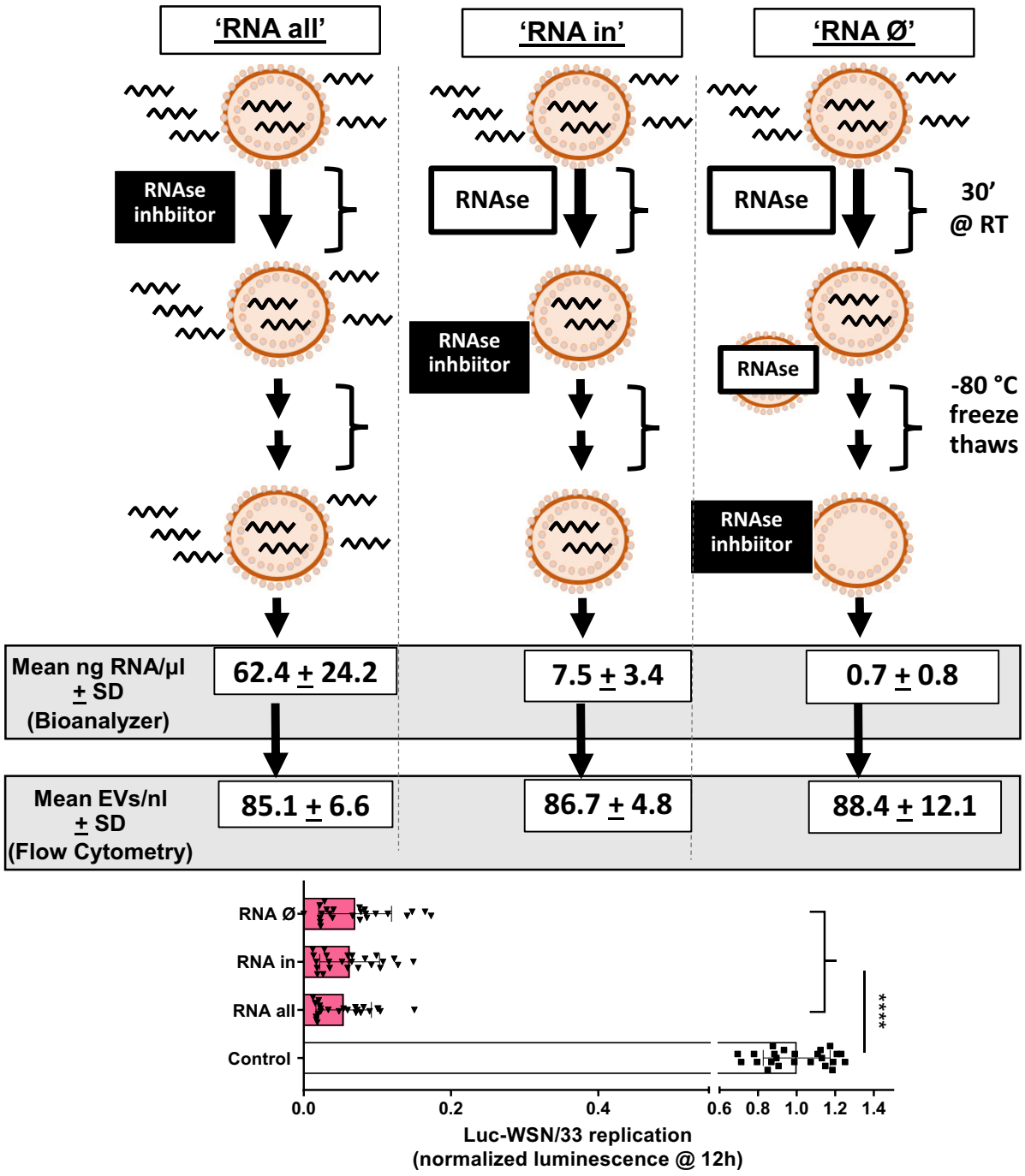

Figure EV2. AM-EV inhibitory activity against influenza is not sensitive to RNase A.

Schematic outline of the strategy to deplete RNA within EVs. Three groups of EVs were isolated from equal volumes of MH-S CM, subsequently treated with either RNase A, and ultimately subjected to gentle permeabilization by repeated freeze-thaw cycles at −80°C to permit RNase A entry into EVs. This permeabilization occurred before (right column) or after (left and middle columns) addition of an RNAse inhibitor. Analysis of EVs in each condition included RNA quantification with Agilent Bioanalyzer 2100 and TapeStation Analysis Software 3.1.1 to quantify the RNA present within EVs ($n = 2$) or quantified with flow cytometry ($n = 2$). These EVs were co-incubated with Luc-WSN/33 in MDCK-SIAT1 cells, and replication was assessed using luminescence. Data represent mean luminescence at 12 h post-infection from individual wells normalized to control from 4 independent experiments.

Data information: Error bars = SD. One-way ANOVA (****P value of < 0.0001).

Source data are available online for this figure.

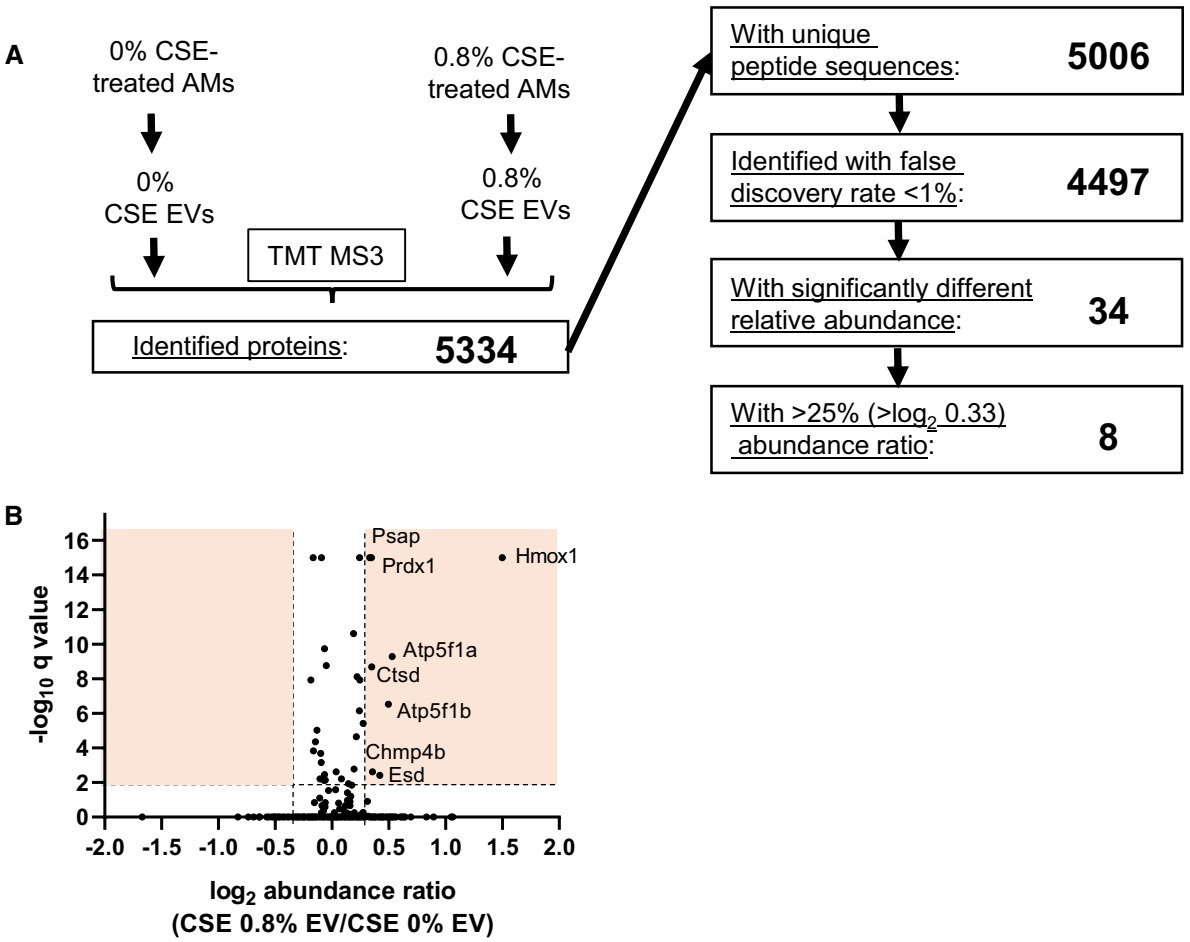

C

Gene Name	Protein	Mean of CSE 0% Group	Mean of CSE 0.8% Group	log2 abundance ratio (CSE 0.8%/CSE 0%)	abundance ratio (CSE 0.8%/CSE 0%)
Psap	Prosaposin	10248	12910	0.333	1.260
Prdx1	Peroxiredoxin-1	30163	38377	0.347	1.272
Ctsd	Cathepsin D	6671	8502	0.350	1.274
Chmp4b	Charged multivesicular body protein 4b	4110	5261	0.356	1.280
Esd	S-formylglutathione hydrolase	3309	4430	0.421	1.339
Atp5f1b	ATP synthase subunit beta, mitochondrial	3942	5562	0.497	1.411
Atp5f1a	ATP synthase subunit alpha, mitochondrial	4245	6134	0.531	1.445
Hmox1	Heme oxygenase 1	1712	4840	1.499	2.827

Figure EV3. Differential abundance of proteins within AM-EVs in response to CSE.

A Flowchart demonstrating the number proteins within each EV condition compared using TMT-MS and each of the listed criteria.

B Volcano plot of all 4,497 proteins identified in both EV conditions. Orange boxes collectively denote the proteins with significantly different relative abundance (a $-\log_{10} q$ value ≥ 2) and with > 25% difference in abundance ratio.

C List of the 8 proteins identified that exhibited > $\log_2$ 0.33 in abundance in EVs isolated from 0.8% CSE-treated AMs compared to 0% CSE-treated AM-EVs.

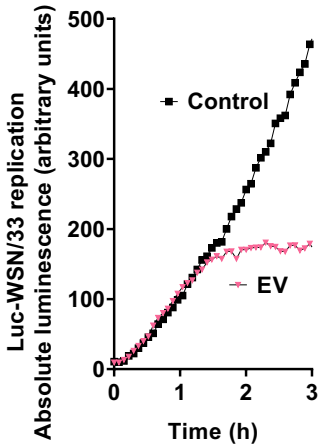

Figure EV4. AM-EVs inhibit Luc-WSN/33 replication within 3 h.

Representative example of measured luminescence from Luc-WSN/33-infected MDCK-SIAT1 cells with (triangles) and without (squares) AM-EVs (EV:cell = 4). Curves shown from this representative experiment display average luminescence reads of 6 wells per condition.

Data information: Mean AUC between curves between 0–1 h were not statistically different, whereas mean AUC between curves 1–3 h were significantly different ($P < 0.0001$, unpaired Student's *t*-test).

Source data are available online for this figure.

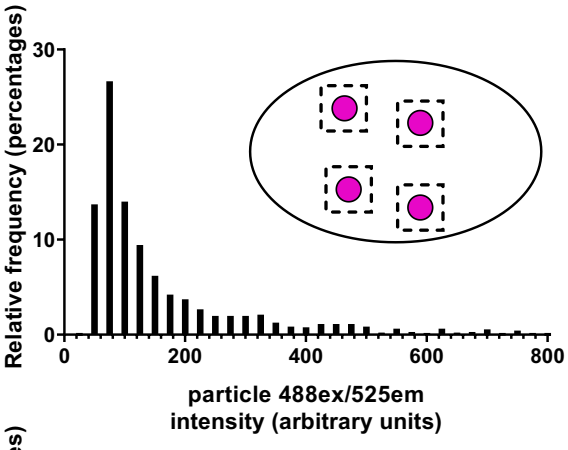

Number of binned values	1422
Minimum	39
25% Percentile	70
Median	104
75% Percentile	192.5
Maximum	1077
Mean	165.43
Std. Deviation	153.57
Std. Error of Mean	4.07
Lower 95% CI of mean	157.44
Upper 95% CI of mean	173.42

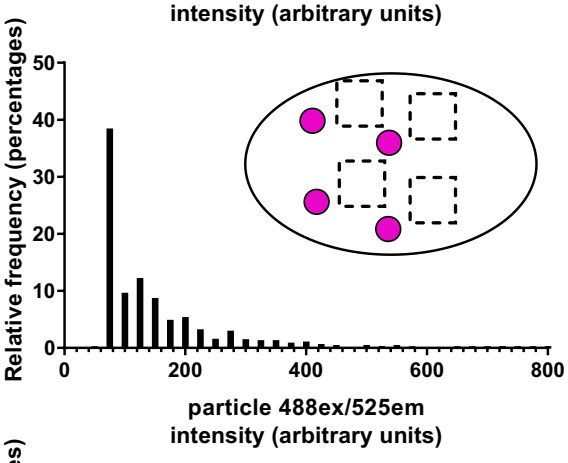

Number of binned values	1624
Minimum	66
25% Percentile	78
Median	114
75% Percentile	190.75
Maximum	1754
Mean	174.44
Std. Deviation	182.33
Std. Error of Mean	4.52
Lower 95% CI of mean	165.57
Upper 95% CI of mean	183.32

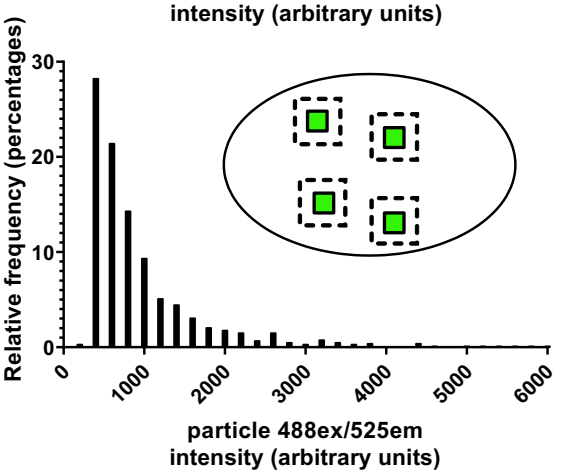

Number of binned values	1085
Minimum	295
25% Percentile	473
Median	698
75% Percentile	1128.5
Maximum	25789
Mean	1049.05
Std. Deviation	1310.47
Std. Error of Mean	39.78
Lower 95% CI of mean	970.99
Upper 95% CI of mean	1127.11

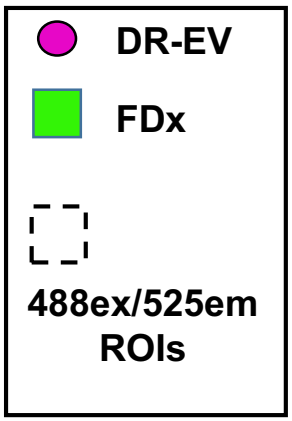

Figure EV5. DR-EVs exhibit no spectral overlap into the emission filter used to detect FDx.

To determine if DR-EVs exhibited spectral overlap with FDx, the emission intensities of DR-EVs (488ex/525em, top histogram) were compared to the background emission intensities (488ex/525em, middle histogram) within MDCK-SIAT1 cells. Using FIJI software, ROIs containing DR-EV particles internalized into MDCK-SIAT1 cells were defined using 647ex/700em images. These ROIs corresponding to DR-EVs were applied to 488ex/525em images to assess their spectral crossover into this emission range, and their corresponding intensities were plotted (top histogram). Particles within the DR-EV ROIs were then cleared from the 488ex/525em images. To establish the background 488ex/525em intensity, new ROIs with the same dimensions were applied to the remaining area within these cells and their associated intensities were recorded and plotted (middle histogram). These histograms show that DR-EVs exhibit no 488ex/525em above background (top vs. middle histogram). For comparison, 488ex/525em intensities of FDx particles were recorded and plotted (bottom histogram). Data represent all measured particles from all cells within 4 hpf per condition. Statistics for each histogram are listed in the figure.